Barkhausen Noise in Magnetic Systems

Li Shu

(Dated: May 8, 2017)

Abstract

Barkhausen noise has attracted growing attentions as an example of complex disordered systems. The renormalization group approach for Barkhausen noise has been developed for the past decades to understand the critical phenomena and applied to other similar systems such as deformation behaviors for solids under tensile stress. In this paper, experimental results and theoretical analysis in the field of Barkhausen noise within a renormalization group framework are reviewed. The discussion of results and future work regarding potential application to other systems are also studied.

I.   INTRODUCTION

When a ferromagnet system is driven by a changing magnetic field, the system jumps from one state with minimum free energy to the next. We observe this process as ferromagnetic materials magnetize. However, many ferromagnets do not magnetize continuously and smoothly, but rather in a series of discrete jumps in different magnetization sizes. The sudden changes in the magnetization of the material produce pulses in the coil around and generate an avalanche detected as a crackling sound, called Barkhausen noise. The phenomena was first observed in 1919.[1] Interestingly, many experiments showed the resulting noise follows power law distributions over several decades in the form of pulse areas and durations.[2,3] Similar scaling behaviors also occur in other systems exhibiting a wide range of avalanches sizes and durations: earthquakes,[4] resistance fluctuations in superconductor,[5] etc.

For the wide similarity between Barkhausen noise in magnet systems and other systems in non-equilibrium state, researchers have been studied Barkhausen noise as an example, hoping to conclude such scaling behaviors to be independent of microscopic details. The successful model could imply all systems mentioned that share the similar behaviors fall within the same universality class. Also, the wide applications of the model enable researchers to translate the similar techniques to understand other complex and non-equilibrium systems such as solids' deformation with the dependence on disorder. One powerful tool to begin this study is the renormalization group (RG) approach.

In this paper, I will briefly explain the modeling of ferromagnets under driving external sources, the use of the RG approach and the scaling collapse and other useful methods used in past research and experimental and simulation results along with their implications.

II.   METHODS

A.   RFIM

To examine the statistical properties of conventional ferromagnets, a hypercubic non-equilibrium zero-temperature random field Ising model (RFIM) is used. The RFIM consists of a lattice of N spins where each spin points up ($s_i = +1$) or down ($s_i = -1$). Spins are under an external magnetic field, $H(t)$ that is changing adiabatically slowly. Similar to the traditional Ising model, spins have nearest neighbors interactions with the parameter J. In this paper, $J = 1$ is used for calculation.

The model also impose a local magnetic field as the local dynamics for spin i, f_i. In real materials, there are always disorder in the form of defects, impurities and other material imperfections. The local magnetic field characterizes these inhomogeneities that result in random anisotropies and varying interaction strengths within the system. We assume a Gaussian distribution[6] for f_i, centered at 0:

$$\rho\left(f_i\right) = \frac{1}{\sqrt{2\pi}R}\exp\left(-\frac{f_i^2}{2R^2}\right),\qquad(1)$$

where R is the standard deviation, corresponding to the disorder level. Disorder leads to the

fact that not all spins will flip homogeneous to the external magnetic field. Instead, they will flip in various avalanche sizes, strongly affected by the local dynamics. Including the random field characterization, the hamiltonian is[6]:

$$\mathcal{H} = -\sum_{i,j} J_{ij} s_i s_j - \sum_i (H + f_i) s_i, \tag{2}$$

Each spin is aligned with its local effective field given as:

$$h_i^{eff} = -\sum_j J_{ij} s_j - H - f_i, \tag{3}$$

The system starts $H(-\infty) = -\infty$ and slowly adiabatically increase from $-\infty$ until the local effective field change the sign when the spin flips.[7] Since the system also includes nearest neighbor interactions, one flipping spin will trigger other spins to flip as well, causing an avalanche. We expect a continuous second order phase transition[8] as follow:

- Zero disorder
  The random field for each spin is the same. If one spin slips and the external field overcomes the interaction in between other spins, all spin will flip. In the hysteresis figure of Magnetization vs External magnetic field, we should expect a sudden jump.

- Infinite disorder
  The random field is significantly different from spin to spin. Each spin will flip independently from the varying magnetic field and have little effects on other spins to flip. Therefore, we should expect a rather smooth hysteresis figure of Magnetization vs External magnetic field.

In between two behaviors above, the phase transition should occur at at some critical value $R = R_c$ where the hysteresis loop exhibits non-analyticity as infinite slope ($\frac{dM}{dH}|_{\pm H_c} \to \infty$), shown in Fig 1[9] below.
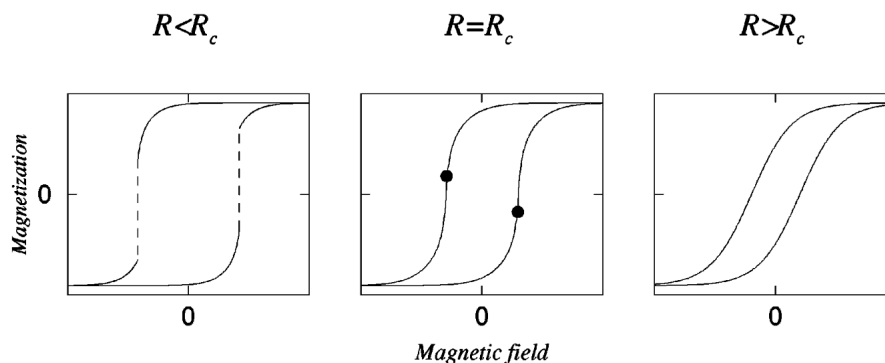

Figure 1: Schematic hysteresis curves for different values of the disorder R. Left: $R < R_c$ (discontinuous hysteresis); center: $R = R_c$ (critical hysteresis); right: $R > R_c$ (smooth hysteresis). For each case, the lower (upper) curve corresponds to an increasing (decreasing) magnetic field.[9]

B.   Mean Field Approximation

The model is solved using Mean Field Approximation that reflects many qualitative features of the scaling behaviors of the system in finite dimensions. The coupling constant J_{ij} is replaced by J/N where we assume that each spin interacts equally with other spins. The Hamiltonian[6] is then:

$$\mathcal{H} = -\sum_i \left(JM + H + f_i \right) s_i, \tag{4}$$

where M is the total magnetization for the system.

As the paper will show later, mean-field theory successfully predicts the critical exponents for systems in six and more dimensions. On the other hand, renormalization group approach will describe the critical exponents in $(6 - \epsilon)$ dimensions for $\epsilon > 0$.

As mentioned earlier, the magnetization per spin should take the following form:[6]

$$M = \int \rho\left(f\right) s_i \, df, \tag{5}$$

$$= (-1) \int_{-\infty}^{-JM-H} \rho\left(f\right) df + (+1) \int_{-JM-H}^{+\infty} \rho\left(f\right) df, \tag{6}$$

$$= 1 - 2 \int_{-\infty}^{-JM-H} \rho\left(f\right) df, \tag{7}$$

The equation above has the following results:

$$R \begin{cases} > \sqrt{\frac{2}{\pi}} J \equiv R_c, & \text{Eq. 7 is analytic for all } H, \\ < \sqrt{\frac{2}{\pi}} J \equiv R_c, & \text{Two stable and one unstable solutions for } M(H) \end{cases} \tag{8}$$

At the critical point $R = R_c$, we observe the diverging slope of $M(H)$. Unlike equilibrium state, non-equilibrium system with no thermal fluctuations is forced by the local dynamics to stay in the current local energy minimum until disrupted by the external field. Therefore, for increasing/decreasing external magnetic field, the system occupies the state with lowest/highest magnetization. Consequently, we observe a hysteresis loop for $M(H)$ with an infinite value of $\frac{dM}{dH}$. We can continue to expand the derivative of M at the critical point, $2J\rho\left(-JM - H\right) = 1$.[6]

$$dM/dH \equiv \chi = [\rho\left(x_c\right)]/\{J[\rho'\left(x_c\right)\left(x - x_c\right) + 1/2\rho''\left(x_c\right)\left(x - x_c\right)^2 + ...]\} \tag{9}$$

where $x_c \equiv -JM(H_c(R)) - H_c(R)$. The integration of Eq. 9 leads to the leading order scaling behavior:[6]

$$M(r,h) \sim |r|^\beta F_\pm \left(h/|r|^{\beta\delta}\right), \tag{10}$$

for small $h = H - H_c(R_c)$ and $r = (R_c - R)/R$ and the mean-field critical exponents $\beta = 1/2$ and $\delta = 3$. $F_\pm$ is given as the smallest real root $g_\pm(y)$ of the equation below,

$$g^3 \mp \frac{12}{\pi} g - \frac{12\sqrt{2}}{\pi^{3/2} R_c} y = 0, \tag{11}$$

where $\pm$ refers to the sign of r.

We continue to make the assumption that, during the interval of random fields $[f_i, f_i + 2S(J/N)]$, the probability density of random fields is approximately constant. A Poisson distribution can be used to characterize the probability for an avalanche of size, S, as:[6]

$$P(S) = \frac{\lambda^{(S-1)}}{(S-1)!}\exp(-\lambda), \tag{12}$$

where $\lambda = 2JS\rho(-JM - H) = S(t+1)$ and $t \equiv 2J\rho(-JM - H) - 1$. Using the probability density function and Stirling's forma, we find the scaling form near the critical point to be[6]

$$D(S, r, h) \sim S^{-\tau}D_{\pm}(S/|r|^{-1/\sigma}, h/|r|^{\beta\delta}), \tag{13}$$

where the mean field scaling function is

$$D_{\pm}(x, y) = \frac{1}{\sqrt{2\pi}}\exp\left(-x[1 \mp \frac{\pi}{4}g_{\pm}(y)^2]^2/2\right), \tag{14}$$

The mean-field critical exponents are calculated as[6]

Table I: Critical exponents from mean-field calculation

Exponents values	Mean Field
τ	3/2
σ	1/2
$\beta\delta$	3/2

C.   Renormalization Group Approach

In order to apply RG methods for RFIM, time parameter, t, is introduced to the problem. External magnetic field now has a time dependence as $H(t) = H_0 + \Omega t$[6], where H_0 is the magnetic field when $t = 0$ and $\Omega > 0$ is the sweeping rate for a monotonically increasing magnetic field. Each spin also takes a double-well potential $V(s_i)$

$$V(s_i) = \begin{cases} \frac{k}{2}(s_i + 1)^2, & \text{for } s < 0, \\ \frac{k}{2}(s_i - 1)^2, & \text{for } s > 0. \end{cases} \tag{15}$$

The partition function Z for the non-equilibrium system is calculated as[10]

$$1 \equiv Z = \int [ds]J[s] \prod_i \delta\left(\partial_t s_i/\Gamma_0 + \delta\mathcal{H}/\delta s_i\right), \tag{16}$$

where Γ_0 is a friction constant in the form as $(1/\Gamma_0)\partial_t s_i(t) = -\delta\mathcal{H}/\delta s_i(t)$. The conditions are imposed because of the similarity to the real magnets: as the external field is increased,

spin flips which reflects the domain wall motions. The role of a partition function could help derive useful exponents and relationships such as the correlation functions. In Ref [6], the investigators employed a coarse-graining procedure as an iterative transformation to calculate different frequency of freedom in the systems to arrive the fixed points.[9]

$$\mathbf{x} \to b\mathbf{x}, t \to b^z t \tag{17}$$

where Ref [6] derived the critical exponents in $(6 - \epsilon)$ dimensions:

$$1/\sigma = z\nu + (2 - \eta)\nu + O(\epsilon^2) = 2 + \epsilon/3 + O(\epsilon^2), \tag{18}$$

$$\tau = 3/2 + O(\epsilon^2), \tag{19}$$

$$\theta\nu = 1/2 - \epsilon/6 + O(\epsilon^2). \tag{20}$$

From RG approach, renormalization-group flows can be constructed to longer length scales. The magnetic model mentioned above, after RG approach, is coarser-grained and removed parts of the degrees of freedom but introduced with different coupling constants.
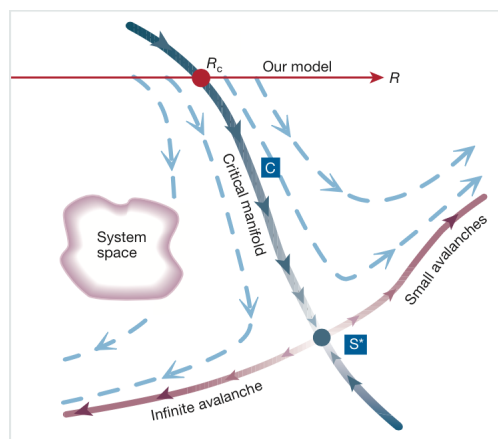

Figure 2: Renormalization-group flows for RFIM model.[11] A fixed point $\mathbf{S}^*$ is self-similar and it has the same scaling behavior on different length scale.

As the we introduce higher level of disorder under the unstable point $\mathbf{S}^*$, the RG flows to the right, which leads to small avalanches. When it flows to the left, the system experience large and possibly infinite-sized avalanche. As it crosses R_c, a phase transition occurs.

Mean-field method also applies here for the soft-spin case. Phase diagram can be constructed using mean-field calculation.[6]
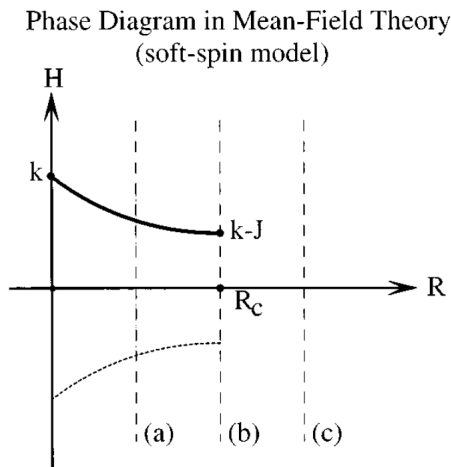
Figure 3: Mean-field phase diagram for the soft-spin model of RFIM. The dash line at (a), (b) and (c) represent three different disorder.[6]

In this case, we observe the non-analyticity at $R = R_c$. Once the disorder cross such critical value, we expect a diverging derivative value of dH/dR. More importantly, the soft-spin model induces history memory for the system. For all values of disorder, hysteresis loop is presented.

D.   Experimental & Numerical Results

From the theoretical calculation using both consistent mean-field theory and renormalization group approach, Ref [11] compares both the numerical and experimental results to theoretical calculation.
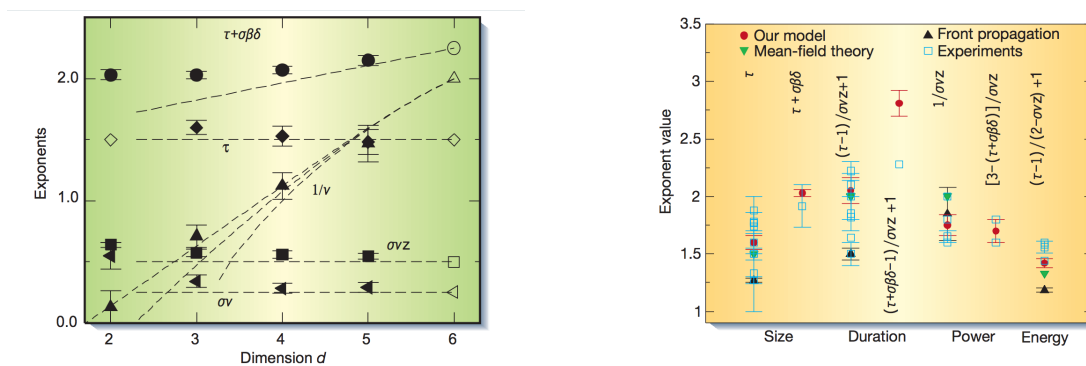

Figure 4: Numerical results and experimental results compared to theoretical calculations. Left: Numerical values (filled dots) of the exponents indicated in figure in 2, 3, 4 and 5 dimensions.The error bars result from the systematic errors from scaling collapse analysis.[11] Right: Comparison between experiments with theory. Different experiments on Barkhausen noise in magnets.[11] "Our model" indicates RG approach. "Front propagation" is not included in this paper.

Figure 3(a) shows the numerical estimates for several critical exponents for multiple

dimensions. As one can see, the results approach mean-field values converge to mean-field predications as the dimension approaches six. This is expected because as the dimension increases, it is more accurate to average fluctuation instead of characterize the pair interaction individually. Moreover, Fig 3(b) shows the RG method is accurate in describing a wide variety of experiments. In order to further test the theory, simulation data is plotted as the avalanche distribution. Using the theoretical calculations above, the critical exponents in 3 dimensions are as follow:
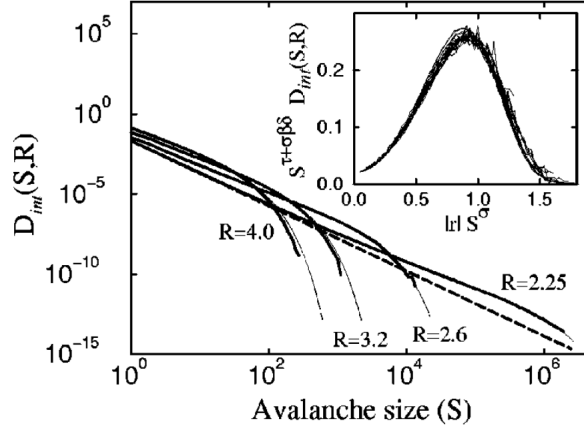

Figure 5: Avalanche size distribution in 3 dimensions integrated over the external field. The system size is 320^3 and the disorders are 4.0, 3.2 and 2.6. Inset: a scaling collapse of the curves in 3 dimensions using the functional form Eq. 13.[12]

In Fig 4, the critical exponents are obtain by using a scaling collapse for different curves. The scaling form is an integrated form[12] of Eq. 13

$$D_{int}(S, R) \sim S^{-(\tau+\sigma\beta\delta)} D_+^{(int)}(S^\sigma|r|) \tag{21}$$

where $D_+^{(int)(X)}, X = S^\sigma|r|$ is a scaling function. Far from the critical point, we observe the power law $S^{-0.23}$. The scaling collapse yields the following exponents values, compared to the mean-field calculation

Table II: Critical exponents in 3 dimensions

Exponents values	RG methods	Mean Field
τ	1.60 ± 0.06	1.5
$1/\sigma\nu z$	1.75 ± 0.07	2

Fig 4 not only provides consistencies between the model and numerical results, but also confirms the fact mean-field approximation is a valid method to model this non-equilibrium system. With the power law for the disorder $R = 2.25$ and increasing magnitude of avalanche sizes, one concludes that Barkhausen noise is a **disorder induced critical point** where the tuning parameter is the disorder value, R.

III.   CONTROVERSY

Despite the self-consistent theory claiming the Barkhausen noise is a disorder induced critical point above, other arguments have been raised to interpret Barkhausen noise differently. In Ref [13], J. S. Urbach, *et al* argued that Barkhausen signal is a self-organized criticality. The argument starts with the observation that Barkhausen noise is strongly affected by a long-range demagnetization field. This effect included to a model of interface depinning will significant change the model behaviors. Interfaces here correspond to the domain walls of flipping spins. Demagnetization results from the magnetic fields from the rest of the spins in the systems. After an increasing field is exerted on an domain interface, the magnetic field should decrease the effective magnetic field at the domain interface. The demagnetization then increases until the effective field is weak for the interface to be pinned down again.

The effect of the long-range demagnetization field can be confirmed through the autocorrelation of the avalanche distribution sequence.[13] During an increase in external magnetic field, a domain wall moves with flipping spins. Meanwhile, the effective field on the domain walls should be decreased. The following event, therefore, is expected to be of a less magnitude when the external field is increased so that the effective magnetic field changes the sign again, which is a consequence of peak repulsion. Therefore, an autocorrelation[13] is useful to determine the claim above
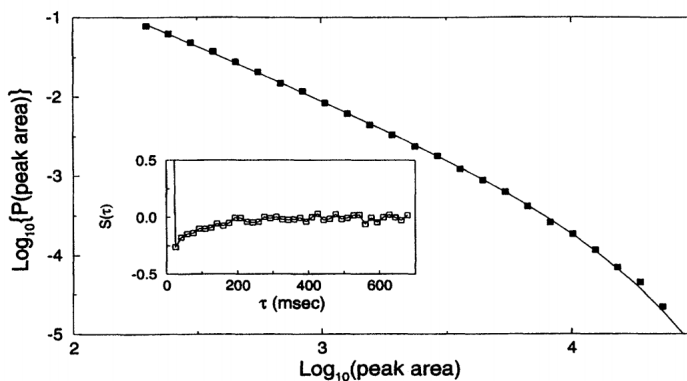

Figure 6: Experimental results on samples containing 30 % Fe, 45 % Fe and 25 % Co of avalanche size that follow a fitting line of $P(A) \propto A^{-\alpha}\exp(-A/A_0)$. Inset: normalized autocorrelation function for the experimental Barkhausen noise.[13]

The dip at the origin indicates avalanches to repel from each other.[13] A numerical result was also presented in Ref [13].
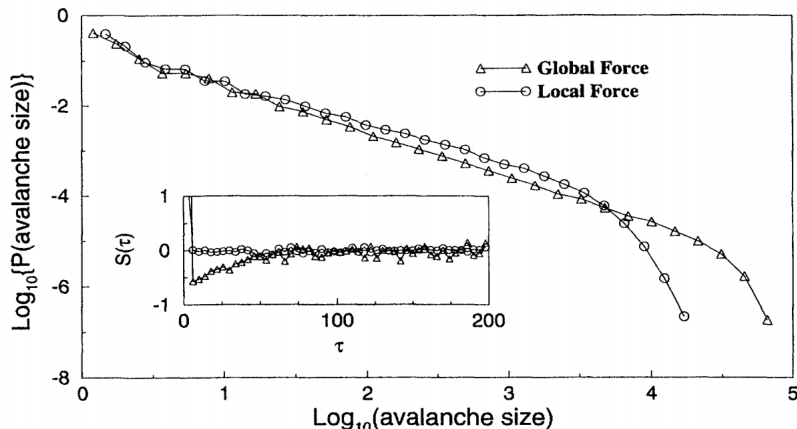
Figure 7: Numerical results for avalanche size probability the local force and global force methods. Inset: normalized autocorrelation function for each model.[13]

The effect of demagnetization is modeled using a global force, as indicated in Fig. 5, in the form as $H_i = H - \eta M$ where η describes the strength of demagnetization field. Local force is then modeled as the local magnetization field, corresponding to disorder in previous methods. As shown in Fig. 6, the addition of demagnetization field produces another dip in simulation, showing that avalanches tend to repel in time series. Local force, on the other hand, does not result in such a dip. One can conclude that the presence of long-range demagnetization field implies self-organized criticality instead of a disorder induced critical point.

IV.   CONCLUSION

From two individual research projects above, different approaches and claims have been made to Barkhausen noise. Both provide consistent numerical and experiment results. Therefore, it is possible that not all ferromagnets behave the same way under varying external fields. For hard ferromagnets and some rare materials, where the microscopic structure limits the formation and motion of domain walls, the first method using RG approach and mean-field calculation is more accurate. For soft ferromagnets in the second method, the depinning model of domain wall is more appropriate for experimental studies. There are numerous promising work to be done in the future. Self-consistency argued by the first method using RG approach and mean-field calculation demands the similar behaviors of other systems within the same universality class. For example, one can study the impurities from solids' deformations under tensile stress using the same approach. Similar to the second method, other ferromagnet materials could be studied. We should expect a wide application for both approaches and investigate the physical details on the regimes where each model applies.

REFERENCES

[1] H. Barkhausen, Z. Phys. **20**, 401 (1919).

[2] P. J. Cote and L. V. Meisel, Phys. Rev. Lett. **67**, 1334 (1991); L. V. Meisel and P. J. Cote, Phys. Rev. B **46** 10 822 (1992).

[3] G. Bertotti, G. Durin, and A. Magni, J. Appl. Phys. **75**, 5490 (1994).

[4] J. Ortin *et al.*, J. Appl. Phys. IV **5**, 209 (1995).

[5] W. Wu and P. W. Adams, Phys. Rev. Lett. **74**, 1206 (1995).

[6] K. Dahmen and J. P. Sethna, Phys. Rev. B. **53**, 14 872 (1996).

[7] M. C. Kuntz and J. P. Sethna, Phys. Rev. B. **62**, 11 699 (1996).

[8] A. P. Mehta, A. C. Mills, K. Dahmen and J. P. Sethna, Phys. Rev. E. **65**, 046139 (2002).

[9] R. Silveira and M. Kardar, Phys. Rev. E. **59**, 1355 (1999).

[10] O. Narayan and D. S. Fisher, and M. Kardar, Phys. Rev. Lett. **46**, 11 520 (1992).

[11] J. P. Sethna, K. Dahmen and C. R. Myers, Nature. **410**, 80 (2001).

[12] O. Perković, K. Dahmen, and J. P. Sethna, Phys. Rev. Lett.**75**, 4528 (1995).

[13] J. S. Urbach, R. C. Madison and J. T. Markert, Phys. Rev. Lett.**75**, 276 (1998).